

# Wetting and Soldering Behavior of Eutectic Au-Ge Alloy on Cu and Ni Substrates

C. LEINENBACH,<sup>1,3</sup> F. VALENZA,<sup>2</sup> D. GIURANNO,<sup>2</sup> H.R. ELSENER,<sup>1</sup>  
 S. JIN,<sup>1</sup> and R. NOVAKOVIC<sup>2</sup>

1.—Empa-Swiss Federal Laboratories for Materials Science and Technology, Laboratory for Joining and Interface Technology, Überlandstrasse 129, 8600 Dübendorf, Switzerland. 2.—National Research Council (CNR), Institute for Energetics and Interphases (IENI), Genoa, Italy. 3.—e-mail: christian.leinenbach@empa.ch

Au-Ge-based alloys are interesting as novel high-temperature lead-free solders because of their low melting point, good thermal and electrical conductivity, and high corrosion resistance. In the present work, the wetting and soldering behavior of the eutectic Au-28Ge (at.%) alloy on Cu and Ni substrates have been investigated. Good wetting on both substrates with final contact angles of 13° to 14° was observed. In addition, solder joints with bond shear strength of 30 MPa to 35 MPa could be produced under controlled conditions. Cu substrates exhibit pronounced dissolution into the Au-Ge filler metal. On Ni substrates, the NiGe intermetallic compound was formed at the filler/substrate interface, which prevents dissolution of Ni into the solder. Using thin filler metal foils (25 μm), complete consumption of Ge in the reaction at the Ni interface was observed, leading to the formation of an almost pure Au layer in the soldering zone.

**Key words:** High-temperature solder, lead-free solder, wetting, soldering

## INTRODUCTION

Sn-Pb alloys have been widely used as important soldering materials in the electronics industry. However, Pb is harmful to both the environment and human health. On the other hand, Sn-Pb alloys would no longer satisfy the reliability requirements and higher mechanical, thermal, and electrical loads in smaller size solder joints during the service of high-power electronic and optoelectronic devices. Hence, increasing efforts have been made to search for suitable high-temperature Pb-free solders to replace the conventional Sn-Pb alloys.<sup>1–3</sup> Au-based alloys fulfill these requirements. The eutectic Au-29Sn (at.%) alloy with melting temperature of 551 K is widely used in the electronics industry, but some applications, e.g., in high-power electronics, require even higher melting temperatures. The Au-28Ge (at.%) eutectic alloy shows an interesting

combination of low melting temperature (634 K), high thermal and electrical conductivity, good mechanical properties, and good corrosion resistance.<sup>4</sup> Moreover, the Au-Ge phase diagram is of the simple eutectic type (Fig. 1).<sup>5</sup> The addition of metals, such as Si, Sn, Sb or In, to the eutectic alloy leads to a further decrease in the melting point.<sup>6–8</sup> Therefore, despite their high cost, Au-Ge-based alloys have been proposed as possible high-temperature lead-free solder materials for highly loaded components such as high-power microelectromechanical systems (MEMS) devices but also in space technology as well as for corrosion-resistant solders for components exposed to aggressive media such as for sensors in corrosive atmospheres and biomedical devices.<sup>9–11</sup>

The soldering process consists in the formation of a joint between the molten solder and a solid metal substrate. The ability of a liquid alloy to flow or spread on the substrate is crucial for the formation of a metallic bond driven by the physicochemical properties of the liquid solder/solid substrate system.<sup>12–14</sup> The spreading of a molten solder over a

(Received November 12, 2010; accepted March 30, 2011;  
 published online April 23, 2011)

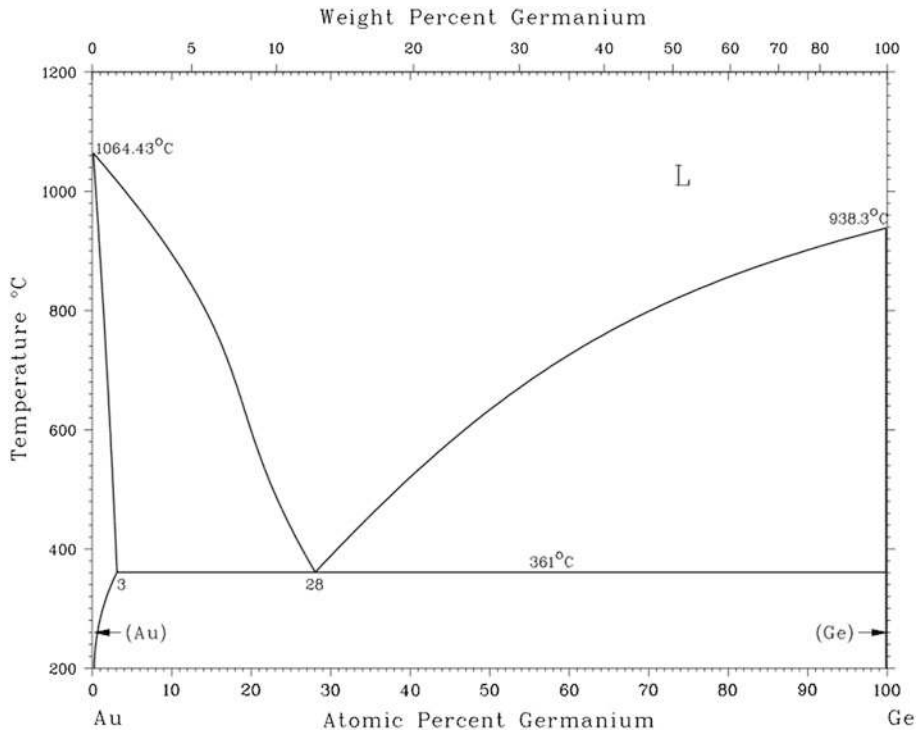


Fig. 1. Au-Ge binary phase diagram.<sup>5</sup> Reprinted with permission of ASM International. All rights reserved. www.asminternational.org.

metallic substrate is a complex problem: it involves many physical and chemical processes,<sup>15</sup> for example, the diffusion between the liquid and solid, and the nucleation followed by the formation and growth of possible intermetallic compounds at the interface, which together determine the behavior of the metal-metal system.<sup>16</sup> Accordingly, the characterization of the wetting behavior, in terms of the contact angle, is an important step in the development of novel solder alloys.

In the case of Au-Ge-based alloys, Cu and Ni are relevant substrate materials, commonly used in the microelectronics. However, very little information about their wetting and soldering behavior is reported in the literature. Stainless steel and Cu could be successfully joined with Au-28Ge, but the interface reactions between the solder and the base materials have not yet been studied.<sup>17</sup> Studies on the wetting kinetics of eutectic Au-Ge on relevant substrates are completely lacking.

In the work reported herein, the wetting behavior of Au-28Ge eutectic alloy in contact with Cu and Ni substrates was characterized. In addition, soldering tests with thin ( $d = 25 \mu\text{m}$ ) solder alloy foils were performed, and the interface reactions as well as the bond shear strengths were investigated.

## EXPERIMENTAL PROCEDURES

### Materials and Specimen Preparation

For wetting tests, Au-28Ge alloy samples of about 1.5 g were prepared from pure components with

purity of 99.99 wt.% (Au, Ge; Alfa Aesar, Karlsruhe, Germany) by arc-melting under a purified argon atmosphere (99.999%) using a nonconsumable tungsten electrode. All samples were melted six times and inverted after three times melting to ensure homogeneity. The cleanliness of the atmosphere was assured by melting a piece of pure Ti as an oxygen getter before melting the Au-Ge alloy samples. In addition, an oxygen cartridge was used in the argon line. Since for the alloy samples the weight loss during melting was less than 0.2 mass%, quantitative chemical analysis of the alloys was not conducted.

Splat-quenched thin foils of eutectic Au-28Ge alloy with thickness of  $25 \mu\text{m}$  (Williams Advanced Materials, Buffalo, USA) were used in soldering tests.

Platelets with thickness of 0.6 mm were produced by laser cutting from pure Cu and Ni sheets (99.99 wt.%; Alfa Aesar, Karlsruhe, Germany) for subsequent wetting and soldering tests. The surface roughness of all platelets was  $R_a = 0.03 \mu\text{m}$ , measured over a length scale of 4.8 mm. For wetting tests, a platelet of  $10 \text{ mm} \times 10 \text{ mm} \times 0.6 \text{ mm}$  in size was used, while soldering tests were performed using small square platelets ( $2 \text{ mm} \times 2 \text{ mm} \times 0.6 \text{ mm}$ ) that were soldered on larger platelets ( $20 \text{ mm} \times 10 \text{ mm} \times 0.6 \text{ mm}$ ).

Prior to all tests, platelets were degassed in a Torvac high-vacuum furnace (Cambridge Vacuum Engineering Ltd., Cambridge, UK) at 773 K and pressure of  $2 \times 10^{-4} \text{ Pa}$  for 1 h. Afterwards, they

were ultrasonically rinsed in ethanol and acetone and dried in air.

### Wetting and Soldering Tests

Wetting behavior was evaluated by contact angle measurements using the sessile drop technique<sup>15</sup> in conjunction with an *ad hoc* designed ASTRAView image analysis software, which allows surface tension, drop dimensions, and contact angle data to be obtained during each experimental run.<sup>18,19</sup> All measurements were performed at  $T = 643$  K and under a reducing atmosphere of Ar-5 vol.% H<sub>2</sub> mixture. To prevent oxidation phenomena with an “oxygen-free” atmosphere, a Zr foil placed over the liquid alloy sample was used as a getter, to further reduce the oxygen content in the surrounding atmosphere. Experiments were carried out in a specially designed furnace,<sup>20</sup> which is made of two concentric horizontal alumina tubes. The pressure inside the inner tube can be kept at less than  $10^{-4}$  Pa using a turbomolecular pump. Alternatively, controlled atmospheres can be introduced inside the working chamber. The oxygen partial pressure of the working atmosphere is continuously monitored by solid-state oxygen sensors at the chamber inlet and outlet. The temperature, monitored by an S-type thermocouple placed just below the specimen, was kept constant within  $\pm 2$  K. The wetting specimen was introduced by a magnetically operated push rod into the preheated furnace only when isothermal conditions were reached. The brazing alloy was melted within 30 s. Resting on a perfectly leveled substrate, the drop/substrate couple was recorded as sharp, back-lit images, using a high-resolution charge-coupled device (CCD), camera and processed using ASTRAView software in a LABview environment. The drop/substrate profile was acquired with precision of  $\pm 1$   $\mu\text{m}$  through careful determination of the magnification factor, while contact angle data were evaluated with accuracy of  $\pm 0.5^\circ$ . After testing, the drop/substrate couple was moved into the colder part of the experimental apparatus and cooled down to room temperature.

Soldering tests were carried out in the above-mentioned high-vacuum furnace (“Materials and Specimen Preparation” section) under pressure of  $2 \times 10^{-4}$  Pa and at temperature of 673 K for dwell time of 10 min using a special soldering jig. Au-Ge foil pieces of about 5 mm  $\times$  5 mm were positioned between the two platelets. The application of a small pressure onto the joint during the soldering process prevented floating and rotating of the top plate and ensured sufficient wetting.

### Characterization Techniques

After the tests, cross-sections of the wetting and soldering specimens were prepared using standard metallographic methods. In both cases, the microstructures were investigated by scanning electron

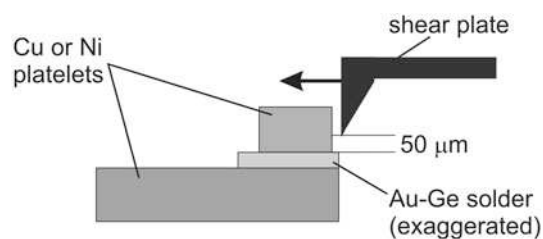


Fig. 2. Schematic of the shear test setup.

microscopy (SEM). The compositions of the phases in the vicinity of the reaction interfaces were analyzed by energy-dispersive x-ray (EDX) analysis.

In addition, microhardness measurements were conducted on the cross-sections of the wetting specimens using a standard Vickers-type diamond tip indenter (Leica VMHT MOT). Special attention was paid to set the indenter properly for the defined specimen surface (bulk alloy and bulk substrate; interface drop/substrate). An optimum load value of 50 mN was chosen, being applied to all samples for 12 s.

The shear strength of the solder joints was determined with a STM-20A shear testing device (Walter + Bai AG Testing Machines, Loehningen, Switzerland). With respect to the shear testing device's design, the load was introduced 50  $\mu\text{m}$  above the interface between the solder alloy and the metal substrate as well as parallel to it. Figure 2 shows a schematic of the setup. The tests were performed under displacement control with shear rate of 0.1 mm/s. The maximum load was obtained from load-displacement graphs and divided by the soldered substrate area ( $A_{\text{substrate}} = 4 \text{ mm}^2$ ) to obtain the shear strength. For both Cu-Cu and Ni-Ni joints, eight tests were performed under ambient temperature. A more detailed description of the shear test setup is given by Siegmann et al.<sup>21</sup>

## RESULTS

### Wetting Behavior of Au-28Ge/(Cu,Ni) Systems

The wetting characteristics of Au-28Ge/Cu and Au-28Ge/Ni systems were determined under isothermal conditions at temperature of  $T = 643$  K for 60 min.

#### *Au-28Ge/Cu*

The variations of the contact angle,  $\theta$ , at  $T = 643$  K as a function of time for the Au-28Ge/Cu system are shown in Fig. 3. The initial contact angle was close to  $52^\circ$ . It started to decrease sharply and reached a constant value of  $\theta = 14 \pm 2^\circ$  in 2 min. After cooling, the sample was metallographically prepared in order to characterize the interface cross-section by SEM and EDX analyses. Close to the Cu substrate, a thick ( $\sim 30$   $\mu\text{m}$ ) interface layer with composition Au-20Cu-6Ge (at.%) was identified (Fig. 4). Adjacent to the solder, Au-13Cu-27Ge

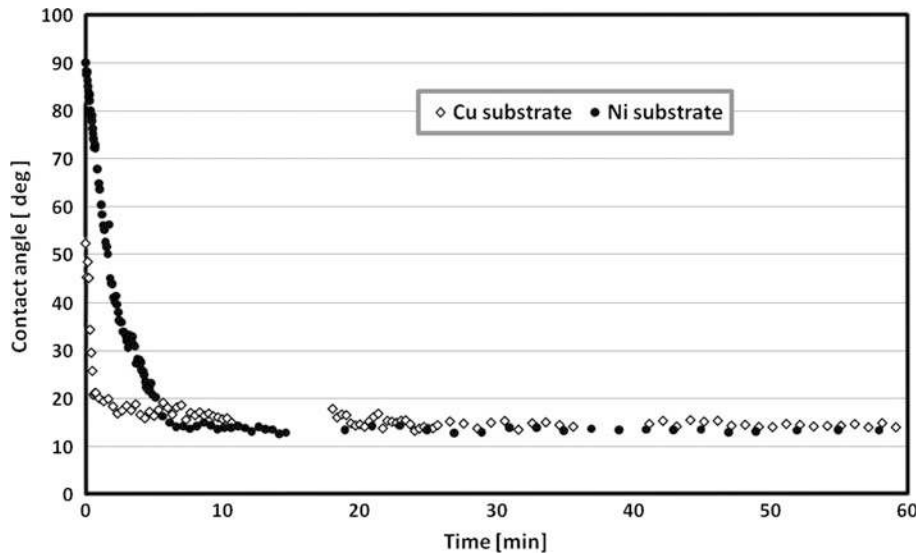


Fig. 3. Contact angle as a function of time for Au-28Ge (at.%) on Cu and Ni substrate.

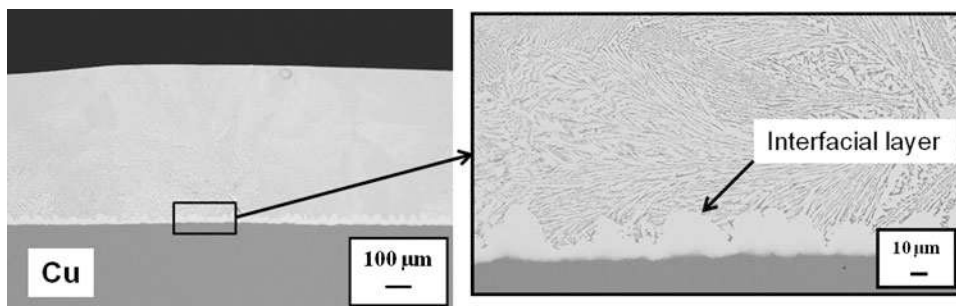


Fig. 4. Au-28Ge (at.%) on Cu: cross-section and formation of reaction layer in the vicinity of the solder/substrate interface.

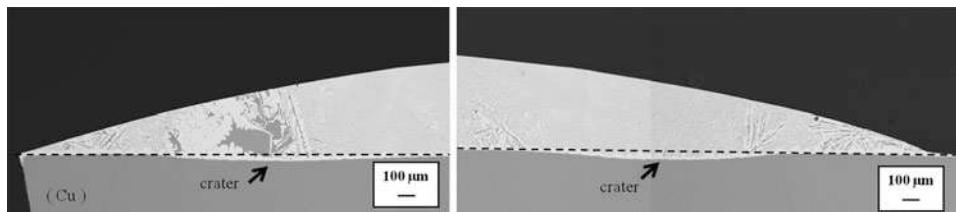


Fig. 5. Au-28Ge (at.%) on Cu: formation of craters in the Cu substrate.

(at.%) bulk phase with eutectic structure was detected.

The reaction between the Au-28Ge alloy and the Cu substrate led to an increase of the total volume of the liquid phase. Due to the pronounced dissolution of Cu into the liquid alloy, the interface was not flat. Indeed, SEM observation of cross-sections of the samples showed that two small craters were formed and the drop extended outside the craters beyond the edges of the Cu substrate (Fig. 5). Moreover, the presence of some spots of Cu in the whole droplet was detected by EDX analysis. The observed wetting behavior can be

classified as dissolutive wetting,<sup>15</sup> thus the final contact angle value,  $\theta = 14 \pm 2^\circ$ , can also be considered as an apparent angle. The morphology of the solidified droplet exhibits a thin “strip” around the droplet with composition of Au-31Cu-6Ge (at.%), while towards the center of the droplet, the morphology changes from a rather irregular shape to a regular one (Fig. 6). The SEM and EDX analyses revealed the Au-14Cu-34Ge (at.%) phase with a eutectic microstructure in the bulk alloy. It is interesting to notice the presence of some large Ge grains close to the surface of the solidified droplet.

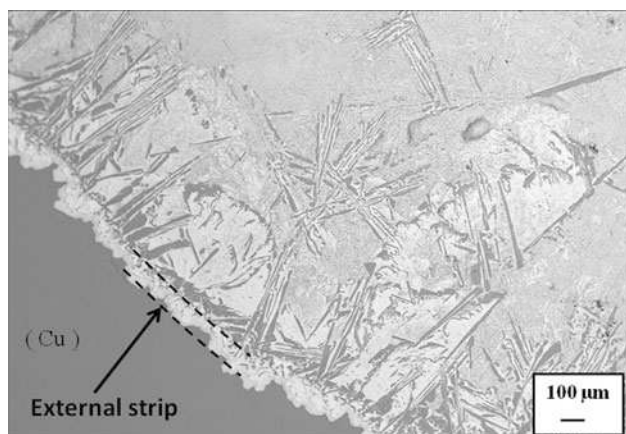


Fig. 6. Au-28Ge (at.%) on Cu: top view morphology of the droplet after solidification.

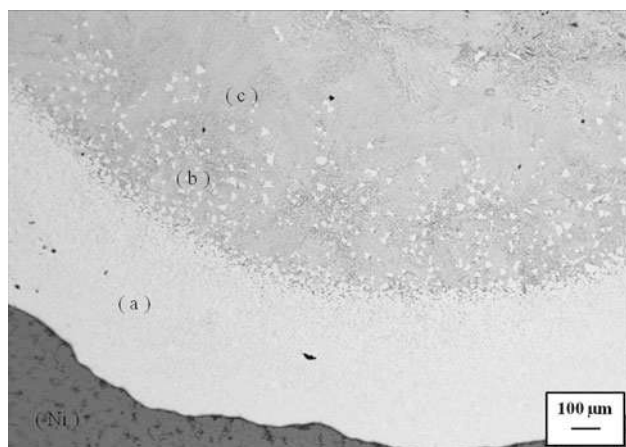


Fig. 7. Au-28Ge (at.%) on Ni: top view morphology of the droplet after solidification with formation of three different zones (a-c).

### Au-28Ge/Ni

The variations of the contact angle at  $T = 643$  K as a function of time for the Au-28Ge/Ni system are shown in Fig. 3. The initial contact angle was about  $90^\circ$ . The rate of change of contact angle with time was lower compared with that observed for the Au-28Ge/Cu system. The final contact angle value of approximately  $\theta = 13 \pm 2^\circ$  for equilibrium conditions was reached after 7 min (Fig. 3).

A top view of the Au-28Ge/Ni system after the wetting test is shown in Fig. 7. Three zones could be clearly distinguished, which are designated as: (a) an Au-rich zone, (b) a transition zone, and (c) an eutectic zone (Fig. 7). The gold-rich zone with thickness  $< 10 \mu\text{m}$  surrounds the droplet. The morphologies of these zones are shown in the cross-section in Fig. 8. In contrast to the tests performed on Cu substrate where pronounced dissolution of Cu was observed, presence of Ni was not observed in the bulk alloy. Moreover, EDX analysis of the cross-section of the specimen showed a very thin, macroscopically planar interface layer ( $5 \mu\text{m}$ ) with composition Ni-(49–50)Ge. Close to this phase, almost pure gold grains were found, as shown in Fig. 8. It can be supposed that the formation of this intermetallic phase (NiGe)<sup>5</sup> probably prevents dissolution of nickel into the liquid alloy.

After the wetting tests, microhardness measurements were conducted on both systems at room temperature. On each sample Vickers microindentations were made at areas of bulk substrates (Ni and Cu), bulk solder alloys, as well as on their interface. The data reported in Table I are average values of ten measurements.

The tests were performed on Au-28Ge/Cu and Au-28Ge/Ni samples within areas visible in the corresponding micrographs (Figs. 4 and 8, respectively).

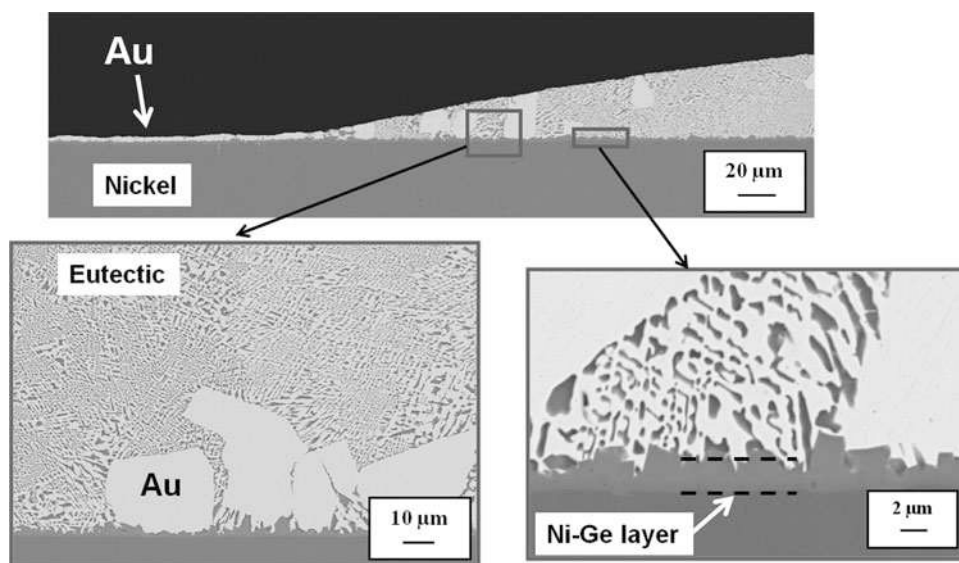


Fig. 8. Au-28Ge (at.%) on Ni cross-section: formation of thin gold layer and gold-rich grains as well as of reaction layer in the vicinity of the solder/substrate interface.

**Table I. Microhardness data for Au-28Ge/(Cu,Ni) samples after wetting experiments**

Test	Phase (at.%)	Au-28Ge/Cu (GPa)	Phase (at.%)	Au-28Ge/Ni (GPa)
Bulk of substrate	Cu	0.539	Ni	1.373
Bulk of alloy	Au-13Cu-27Ge	1.971	Au-28Ge	2.295
Interface	Au-20Cu-6Ge	1.098	Ni-50Ge	1.128

The microhardness results indicated generally lower values in the case of Au-28Ge/Cu. The two interfaces are characterized by the presence of gold: a discontinuous, thick layer of the gold-rich phase [Au-20Cu-6Ge (at.%); Fig. 4] and a coarser layer of almost pure gold grains close to a thin interface layer of an intermetallic phase [Ni-(49–50)Ge (at.%); cf. Fig. 8], which exhibits similar microhardness values (Table I). On the other side, fast diffusion of copper into the interface and through the bulk solder alloy contributes to the formation of Cu-containing ternary phases with eutectic microstructure that exhibits lower microhardness than the corresponding phase in Au-28Ge/Ni samples. Interestingly, the NiGe reaction layer appears to be relatively soft.

### Soldering Behavior of Au-28Ge/(Cu,Ni) Systems

Figure 9a, b show a top view and cross-section of a Cu-Cu specimen after soldering. In Fig. 9a only slight soldering of the Au-28Ge foil after soldering can be seen; the area covered by the filler metal is about the same as the dimensions of the piece of foil that was positioned between the platelets prior to brazing. In addition, the solidified filler metal appeared with a grey color instead of the golden color of the filler metal foil. The cross-section in Fig. 9b shows the microstructure of the soldering zone after the soldering test. Despite the fact that the solder foil had thickness of only 25  $\mu\text{m}$ , the width of the soldering zone is about 50  $\mu\text{m}$  after the test. In contrast to the results of the wetting tests, no eutectic microstructure was observed. Ge-rich grains with approximately 10 at.% to 15 at.% Au were found along the centerline of the soldering zone. They are embedded in a matrix with composition of approximately Au-30Cu-6Ge (at.%). At the interfaces, a layer with thickness of 2  $\mu\text{m}$  to 3  $\mu\text{m}$  and composition of Au-64Cu-12Ge (at.%) formed. In the vicinity of the interfaces, amounts of Au up to 13 at.% were detected in the Cu substrate.

Figure 10a, b shows corresponding images for a Ni-Ni specimen. The spreading of the solder material was rather extensive, as can be seen in Fig. 10a. The area covered by solidified solder material is significantly larger than the initial solder foil dimensions, which are indicated by dashed lines.

Figure 10b shows a SEM micrograph of the cross-section after soldering. It can be seen that the solder gap width is only about 5  $\mu\text{m}$  to 6  $\mu\text{m}$ . The bright

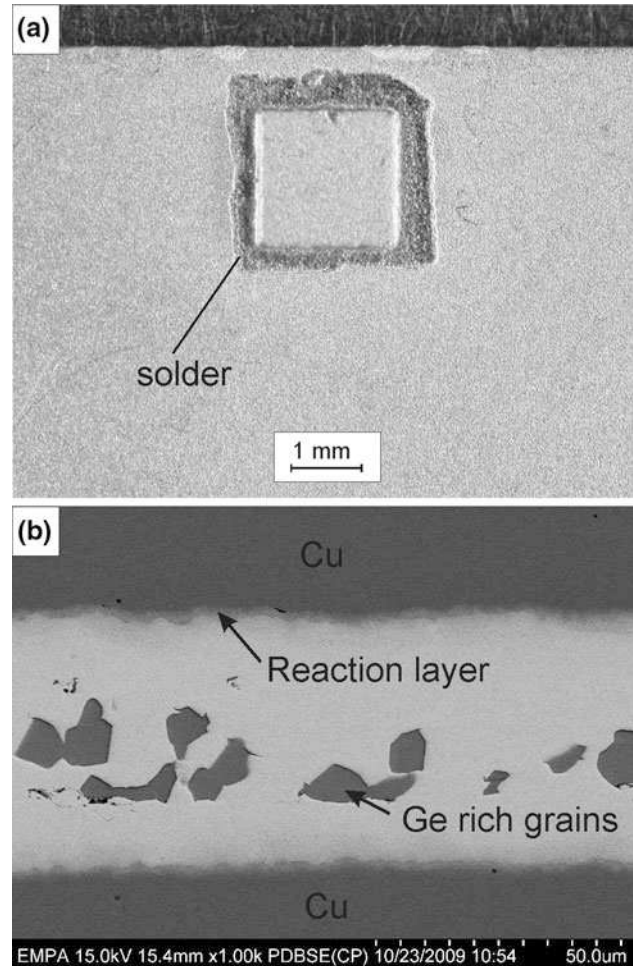


Fig. 9. (a) Top view of Cu-Cu solder joints and (b) SEM cross-section of interface microstructure of Cu-Cu solder joints.

layer consists mainly of Au (>96 at.%) with some minor amounts of Ni and Ge. In addition, reaction layers with thickness of 2  $\mu\text{m}$  to 3  $\mu\text{m}$  and composition Ni-(49–50)Ge (at.%) formed at both interfaces.

The wetting characteristics of a melt/substrate system are usually the key parameters used to define soldering tests. In the present work, the spreading kinetics of both systems are similar after 10 min and the resulting contact angle values are close to each other (Fig. 6). Therefore, after the soldering tests, the corresponding spreading areas differ significantly (Figs. 9, 10), probably due to the formation of the Au-rich layer in the case of the Ni substrate. Indeed, there are many examples in the

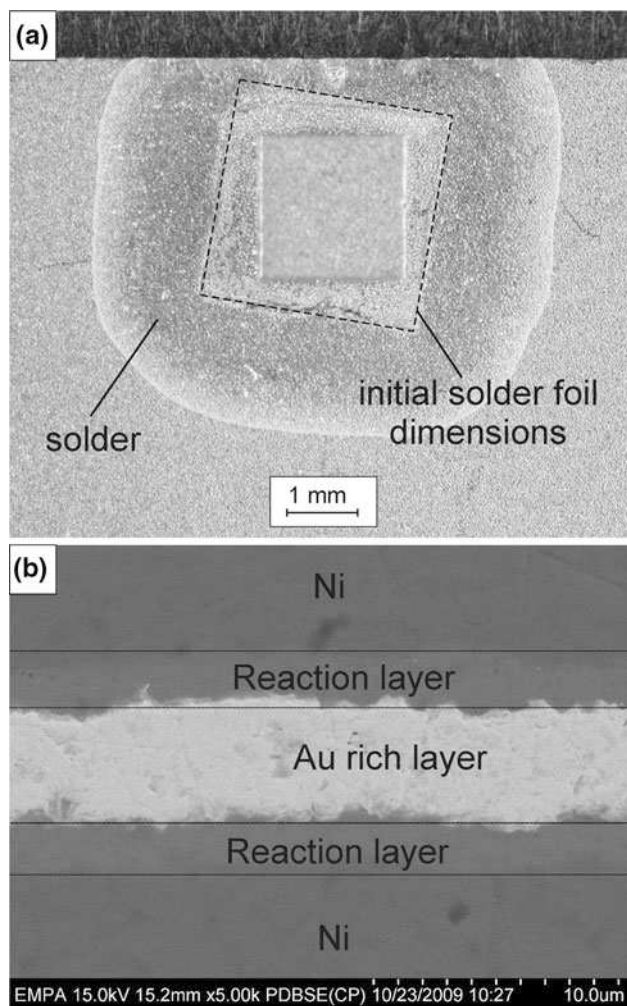


Fig. 10. (a) Top view of Ni-Ni solder joints and (b) SEM cross-section of interface microstructure of Ni-Ni solder joints.

literature concerning so-called gold-plated substrates,<sup>9</sup> used to improve the wetting characteristics of solders and brazes.

In Table II, the results of the shear tests on the Cu-Cu and Ni-Ni solder joints are summarized. Beside the maximum and minimum shear strength values, the mean shear stresses at specimen failure as well as the standard deviations are given. Rather similar values of the mean shear strength of approximately 30 MPa to 34 MPa were measured for the Cu-Cu and Ni-Ni joints. In addition, the scatter of the shear strength values was more

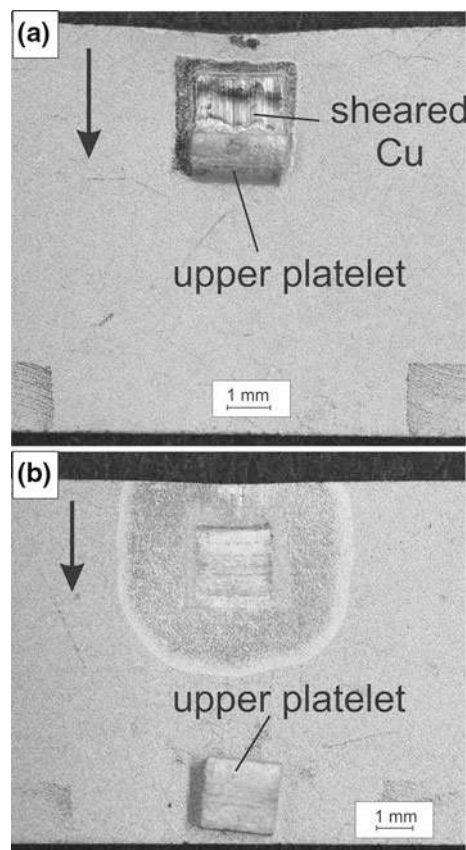


Fig. 11. Solder specimens after shear testing: (a) Cu-Cu specimens and (b) Ni-Ni specimens.

pronounced for the Ni-Ni joints than for the Cu-Cu joints, and maximum values of 50 MPa were measured. The failure mechanisms, however, were different, as can be seen in Fig. 11. While all Ni-Ni joints clearly failed in the joining zone, the Cu-Cu joints failed by pronounced plastic deformation of the upper Cu platelet.

## DISCUSSION

The wetting of liquid Au-28Ge solder alloy in contact with a Cu substrate reveals pronounced dissolution of Cu and fast diffusion of Cu into the liquid solder.

The presence of two small craters which was evidenced by cross-sectional observations on Au-28Ge/Cu samples suggests that the dissolution of the substrate occurred mainly at the triple line

Table II. Results of shear tests after soldering

Joint	No. of Tests	$\tau_{\max}$ (MPa)	$\tau_{\min}$ (MPa)	$\tau_{\text{mean}}$ (MPa)	Standard Deviation (MPa)
Cu-Cu	8	38.9	22.8	34.4	5.1
Ni-Ni	8	50.1	13.1	30.0	12.9

after the initial nondissolutive stage of wetting. Subsequently, the drop extends outside those craters to the edge of the Cu substrate, and further spreading of the ternary saturated alloy [Au-20Cu-6Ge (at.%)] occurred. The formation of an excess amount of the liquid phase results in excessive growth of the interface.

The higher spreading rate for the Au-28Ge/Cu samples compared with those of Au-28Ge/Ni can be explained by invoking the dissolution of the substrate.<sup>22</sup> When dissolution starts, surface tension gradients arise in the liquid: at the interface, where the liquid is enriched in Cu, the surface tension is supposed to be higher than at the top of the droplet, where Au-28Ge is still almost pure.<sup>23</sup> Thus, these gradients cause the liquid to flow from the top to the triple line because of the Marangoni effect, and the spreading rate is enhanced.

On the contrary, in the Au-28Ge/Ni couples no dissolution of the substrate was observed, but a thin reactive intermetallic layer, most likely NiGe with B3<sub>1</sub> structure, formed, which prevented further dissolution of the substrate into the liquid phase.

The results of the soldering tests with Cu substrates lead to the assumption that the increase of the solder gap width after soldering is also due to the pronounced dissolution of the Cu substrates. The enrichment of the solder material with Cu obviously also led to the change of color from gold to grey after soldering.

The results of the solder tests with Ni substrates indicate that a significant amount of solder material has flowed out of the soldering zone between the platelets and has spread over the bottom substrate. Thereby, the solder gap width was decreased.

The explanation of the interface processes is difficult since no phase diagram information is available for the Au-Cu-Ge or Au-Ge-Ni ternary systems. However, no or only little amount of third element was detected in the reaction layers, and the information from the binary systems might be useful for such interpretation.<sup>5</sup>

The compositions of the interfacial layers between Cu substrates and the Au-Ge filler were Au-20Cu-6Ge (at.%) in the case of the wetting specimens and Au-64Cu-12Ge (at.%) in the case of the solder specimens. Since no further phase analysis was performed, e.g., by x-ray diffraction techniques, the structure of the reaction layers remains unclear. According to the binary Au-Cu phase diagram it could be that the reaction layers consist of the Au<sub>3</sub>Cu and the AuCu<sub>3</sub> low-temperature ordered phases, both with L1<sub>2</sub> structure and large solubility range. However, since the processing times were relatively short, the layers are likely a Au-Cu solid solution. The different amounts of Au can be explained with the larger volume of Au-Ge alloy and the larger absolute amount of Au in the wetting tests compared with the soldering tests, where only thin foils were applied. It appears that pronounced diffusion of Cu and Au through the layer takes

place, leading to the observed dissolution of Cu in the liquid Au-Ge alloy as well as to the pronounced Au enrichment of the substrate in the vicinity of the interface. According to the study of Heumann and Rottwinkel,<sup>24</sup> both the intrinsic and the tracer diffusion coefficients of Cu in Cu-rich Au-Cu solid solutions are significantly larger than the corresponding values for Au. This would explain why a very high amount of Cu is present in the solder layer compared with the lower amount of Au in the substrate.

In the case of the eutectic Au-Ge on Ni, Ge has a high driving force to migrate towards the interface, forming a NiGe reaction layer. Diffusion of Ni and Au through this line compound is obviously hindered, and no dissolution takes place.

On the other side, after both tests, only in the case of the Au-28Ge/Cu system, the segregation of Ge has been revealed by EDX/SEM analyses. The corresponding phase diagrams of the Cu-Ge and Ge-Ni systems exhibit three and nine intermetallic compounds, respectively.<sup>5</sup> The existence of intermetallic compounds in the solid state implies the presence of heterocoordinated clusters or aggregates in the liquid phase that affect surface segregation. Thus, the segregation of Ge is related to weak effects of the short-range order in the Cu-Ge liquid phase. On the contrary, pronounced effects of the short-range order phenomena, such as in Ge-Ni melts, may reduce the degree of surface segregation.<sup>13</sup> It is therefore conceivable that Ge-Ni pairing may exist at the liquid surface, and compete with segregation.

Indeed, in solder specimens, the absolute amount of Ge in the soldering zone is relatively low because only a 25 μm thin solder alloy foil was used. In addition, the diffusion distances for Ge are very short. As a consequence, almost all Ge migrated to the interfaces and was consumed by the formation of the above-mentioned reaction layers, leaving a thin layer of almost pure Au. This depletion of Ge obviously also took place during the wetting tests at the edges of molten Au-Ge alloy, where it is rather thin. Since the melting point of the thin Au layer as well as the one of the NiGe reaction layer are significantly higher than the melting point of eutectic Au-28Ge, it can be assumed that isothermal solidification took place during the soldering process. This means that soldering of Ni with a sufficiently thin eutectic Au-28Ge solder alloy is a transient liquid-phase (TLP) bonding process with relatively short processing times. It might therefore be interesting for technical applications, since the remelting temperature of the solder joint is significantly higher than the processing temperature (643 K to 673 K).

The different reactions during soldering led to different failure behaviors of Cu-Cu and Ni-Ni joints during the shear tests. For Cu-Cu joints the bond strength was obviously higher than the yield strength of copper, which is in the range of 70 MPa for tensile loading. Taking into account the von



Mises criterion, the corresponding value for pure shear loading is approximately one half of this value, i.e., 35 MPa. The measured values of 34 MPa can therefore be considered as a lower bound for the bond strength. For the Ni-Ni joints, the limiting parameter is the yield strength of the pure gold layer in the joining zone, which is in about the same range as the yield strength of Cu. This explains the similarity of the shear strength values. For comparison, the strengths of Cu-Cu joints soldered with different Sn-Pb or Sn-Ag-(Cu,Ni) solders were reported to be in the range of 30 MPa to 70 MPa for shear loading and 60 MPa to 85 MPa for tensile loading.<sup>25-28</sup> The values determined in this work can therefore be considered as acceptable for technological applications.

### CONCLUSIONS

Wetting and soldering tests with eutectic Au-28Ge (at.%) alloys and Cu and Ni substrates were performed. Although for both systems similar values of the contact angle were obtained, fundamental differences in the wetting behavior of liquid Au-28Ge eutectic alloy in contact with Cu and Ni substrates were immediately apparent. Their behavior changed from dissolutive wetting, characterized by the formation of a thick interface layer, to a macroscopically planar, thin layer formation, respectively. To reduce the large quantity of liquid phase formed due to the high reactivity between Au-28Ge solder and Cu substrate that results in excessive growth of the interface, it is very important to control and optimize the joining process parameters, such as temperature, surrounding atmosphere, purity of materials, and, in particular, time.

Cu-Cu and Ni-Ni solder joints with joint strengths in the range of 30 MPa to 35 MPa could be successfully produced with the low-melting Au-28Ge alloy. In the case of Cu, pronounced dissolution of the substrate into the liquid led to an increase of the solder gap width from initially 25  $\mu\text{m}$  to 50  $\mu\text{m}$ . On Ni substrates, pronounced spreading of the filler metal was observed. A thin layer of almost pure Au was observed in the soldering zone, which is assumed to have formed by isothermal solidification due to depletion of Ge, which is consumed in the interface reactions.

These results make use of eutectic Au-28Ge alloy as a high-temperature solder alloy interesting for joining of Cu and Ni. In particular, joining with Au-28Ge is interesting in the case of Ni components exposed to elevated temperatures, since the remelting temperature of the solder joint is significantly higher than the processing temperature (643 K to 673 K).

### ACKNOWLEDGEMENTS

This work was financially supported by the Swiss State Secretariat for Education and Research (SBF No. C08.0031) within the European COST action MP0602: "Advanced Solder Materials for High Temperature Application (HISOLD)." The authors thank Dr. A. Passerone, IENI-CNR Genoa, for helpful discussions on this subject.

### REFERENCES

1. K. Zeng and K.N. Tu, *Mater. Sci. Eng. R* 38, 55 (2002).
2. C.M.L. Wu, D.Q. Yu, C.M.T. Law, and L. Wang, *Mater. Sci. Eng. R* 44, 1 (2004).
3. T. Laurila, V. Vuorinen, and J.K. Kivilahti, *Mater. Sci. Eng. R* 49, 1 (2005).
4. D.M. Jacobsen and G. Humpston, *Gold Bull.* 22, 9 (1989).
5. B. Massalski, *Binary Alloy Phase Diagrams* (Metals Park, OH: ASM, 1990).
6. J. Wang, C. Leinenbach, and M. Roth, *J. Alloys Compd.* 485, 577 (2009).
7. J. Wang, C. Leinenbach, and M. Roth, *J. Alloys Compd.* 481, 830 (2009).
8. V. Chidambaram, J. Hald, and J. Hattel, *J. Alloys Compd.* 490, 170 (2010).
9. W.S. Rapson and T. Groenwald, *Gold Usage* (New York: Academic, 1978).
10. H. Takiguchi, Z. Yoshikawa, H. Miyazaki, Y. Okamoto, and J. Morimoto, *J. Electron. Mater.* 39, 9 (2010).
11. T.S. Abhilash, C.H. Ravi Kumar, and G. Rajaram, *Thin Solid Films* 518, 5576 (2010).
12. V. Vuorinen, T. Laurila, H. Yu, and K. Kivilahti, *J. Appl. Phys.* 99, 23530 (2006).
13. R. Novakovic, E. Ricci, F. Gnecco, D. Giuranno, and G. Borzone, *Surf. Sci.* 509, 230 (2005).
14. F. Gnecco, E. Ricci, S. Amore, D. Giuranno, G. Borzone, G. Zanichchi, and R. Novakovic, *Int. J. Adhes. Adhes.* 27, 409 (2007).
15. N. Eustathopoulos, M.G. Nicholas, and B. Drevet, *Wettability at High Temperatures*, Vol. 3 (Oxford: Pergamon Materials Series, 1999).
16. J.A. Warren, W.J. Boettinger, and A.R. Roosen, *Acta Mater.* 46, 3247 (1998).
17. F.M. Hosking, J.J. Stephens, and J.A. Rejent, *Weld. J.* 78, 127 (1999).
18. L. Liggeri and A. Passerone, *High Technol.* 7, 82 (1989).
19. M. Viviani, *ICFAM-CNR Technical Report* (Italy: CNR Genoa 1999).
20. F. Valenza, M.L. Muolo, and A. Passerone, *J. Mater. Sci.* 45, 2071 (2010).
21. S. Siegmund, M. Dvorak, H. Gruetzner, K. Nassenstein, and A. Walter, *Proceedings of the International Thermal Spray Conference*, Vol. 823 (Dusseldorf, Germany: ASM International/DVS, 2005), p. 823.
22. O. Kozlova, R. Voytovych, P. Protsenko, and N. Eustathopoulos, *J. Mater. Sci.* 45, 2099 (2010).
23. Yu.V. Naidich, V.M. Pervtilo, and L.P. Obushchak, *Poroshkovaya Metall.* 5, 73 (1975).
24. T. Heumann and T. Rottwinkel, *J. Nucl. Mater.* 6970, 567 (1978).
25. Y.H. Lee and H.T. Lee, *Mater. Sci. Eng. A* 444, 75 (2007).
26. V. Sivasubramaniam, M. Galli, J. Cugnoni, J. Janczak-Rusch, and J. Botsis, *J. Electron. Mater.* 38, 19 (2009).
27. A. Kar, M. Ghosh, A.K. Ray, and R.N. Ghosh, *Mater. Sci. Eng. A* 459, 69 (2007).
28. K.H. Prakash and T. Sritharan, *Mater. Sci. Eng. A* 379, 277 (2004).